Articles

Chinese Science Bulletin

Materials Chemistry

April 2010 Vol.55 No.10: 921–926
doi: 10.1007/s11434-010-0061-2

# Preparation and properties of CdS/Au composite nanorods and hollow Au tubes

YANG ZhaoHui, CHU HaiBin, JIN Zhong, ZHOU WeiWei & LI Yan*

*Beijing National Laboratory for Molecular Sciences, Key Laboratory for the Physics and Chemistry of Nanodevices, College of Chemistry and Molecular Engineering, Peking University, Beijing 100871, China*

Received March 10, 2009; accepted October 12, 2009

1-dimensional (1D) metal-semiconductor nano-scale composite superstructures based on Au nanoparticles and CdS nanorods were prepared. The outer surface of CdS nanorods was modified with mercapto-ethylamine (MEA) in advance. With the aid of MEA, dense and uniform Au nanoparticles were deposited onto the external wall of CdS nanorods through *in situ* chemical reduction of $AuCl_4^-$ ions. Those Au nanoparticles induced further electroless deposition and a continuous layer of Au was formed on CdS nanorods. Stable hollow Au tubes were obtained after the inner CdS cores were etched by HCl. UV-Vis, FL, XPS, EDX, TEM and SEM measurements were carried out to characterize the produced materials. The quenching of the defect emission of CdS in CdS-nanorod/Au-nanoparticle hybrid superstructures was detected, which was ascribed to the energy transfer from the exciton of CdS to surface plasma resonance level of Au.

**Au nano particles, CdS nanostructures, energy transfer**

**Citation:** Yang Z H, Chu H B, Jin Z, et al. Preparation and properties of CdS/Au composite nanorods and hollow Au tubes. Chinese Sci Bull, 2010, 55: 921–926, doi: 10.1007/s11434-010-0061-2

Hybrid superstructures made of various nano-scaled components have shown unique properties and attracted much attention in recent years [1]. 1-dimensional (1D) nanostructures such as nanorods, nanowires, nanotubes and nanobelts are of special interest because they can act as both functional and connective components in nanodevices and other applications [2–4]. By tailoring nanoparticles and the 1D nanostructure together, the resultant hybrid superstructures can show unique properties. For example, much attention has been paid to the combination of nanoparticles with carbon nanotubes to form nanotube/nanoparticle composites [5–7]. Another interesting example is the assembly of CdSe and Au nanoparticles on the surface of $LiMo_3Se_3$ nanowires through the hydrophobic interaction, which resulted in unique optical and electronic properties [8]. Heterostructures of metal nanoparticles on nanowires have been constructed by electrodeposition [9]. Besides, bio-inspired methods have also been used to fabricate the nanoparticle-nanowire superstructures [10–12].

*Corresponding author (email: yanli@pku.edu.cn)

II-VI group semiconductor materials are very attractive because of their wide applications in light-emitting devices, nonlinear optics, biological labels and photo-electron transfer devices [4,13–15]. On the other hand, spherical noble metal nanoparticles, such as Au and Ag, have also attracted much attention. Due to their unique properties in surface plasma resonance (SPR) and surface enhanced Raman scattering (SERS) [16–18], they are considered as potential components in highly compacted optoelectronic and nonlinear optical devices as well as sensors [19]. When the noble metal nanoparticles and semiconductors were combined together, the complexes would show more interesting properties. Nogami and coworkers found the resonant energy transfer and increase of the two-photon absorption coefficient in Au/CdS composites [20]. Yang et al. [21] reported the enhancement of third-order optical nonlinearity in dens-ely packed Au/CdS composite films. Tang et al. [22] assembled the CdSe/CdS core-shell quantum dots on a chemically modified Au surfaces for photoreception uses. Granot et al. [23] prepared CdS semiconductor nanoparticle monolayer on Au surfaces for photoelectron-chemical

applications. Therefore, it should be very interesting to assemble noble metal nanoparticles on II-VI group semiconductor nanorods and study the property of such 1D superstructure.

Up to now, there are only two examples introducing the nanostructures composed of CdX nanorods (X=S, Se, Te) and noble metal nanoparticles. One comes from Mokari's group, who reported the nano-dumbbell structure of Au/CdSe nanorods through anisotropic selective growth of gold tips onto CdSe nanorods [24]. They found an obvious emission quenching and the increase of the conductivity for CdSe nanorods. The other example comes from Kotov's group. They synthesized CdTe/Au composite nanorods with a dense Au shell through bio-conjugation reaction and found an enhancement of emission related to the long-distance interaction between the semiconductor and the metal [25]. Both cases indicate that the interaction between CdX and metal nanoparticles depends greatly on the band gap of CdX components. Up to now, there is no report about the CdS nanorod/Au nanoparticle complex.

In this paper, we introduced a simple and efficient way to deposit Au nanoparticles onto the sidewall of surface-modified CdS nanorods. A homogeneous and dense layer of Au nanoparticles were successfully assembled onto the positively charged surfaces of the CdS nanorods. This layer of Au nanoparticles can be further developed into Au thin films. The fluorescence and absorbance property of the composites was also studied.

## 1 Experimental

All the reagents and solvents are of analytical grade and used as received.

The CdS nanorods were prepared with the method reported in our previous work [26]. CdS nanorods with an average length of ~750 nm and the diameter of ~35 nm were prepared. The preparation of CdS nanorods capped with Au nanoparticles and the hollow Au tubes was depicted in Scheme 1.

Mercapto-ethylamine (MEA) was used to modify the surface of CdS nanorods. 10 mg CdS nanorods were dispersed in 5 mL MEA aqueous solution (MEA:CdS=2.4:1 mol/mol). The pH of the mixture was adjusted to 6.0, and the mixture was stirred continuously for 4 h. After centrifugation and rinsed with deionized water thoroughly, the MEA modified CdS nanorods were re-dispersed in water.

1 mL aqueous dispersion of as-modified MEA-CdS nanorods (0.2 mg/mL) was mixed with 5 mL $HAuCl_4$ aqueous solution (0.02 mol/L) and stirred for 1 h at room temperature. After centrifugation and washing, the residue was re-dispersed in 10 mL water containing 2 mg $NaBH_4$ and stirred for 30 min. The products were centrifuged and washed thoroughly.

Those Au nanoparticles were used to induce the further electroless deposition of Au. 1 mL $HAuCl_4$ solution (0.2 mol/L) and 1 mL CdS nanorod/Au nanoparticle dispersion (0.2 mg/mL) were mixed in 10 mL water. Under magnetic stirring, 10% $Na_2CO_3$ aqueous solution was added to adjust the pH to 9–10. After stirred for 20 min, the product was separated and washed with deionized water.

Then the product was etched with hydrochloric acid to remove the CdS core. HCl solution of 4.8 mol/L was used. After stirred for 2 h, the product was separated by centrifugation. Then the dissolving process was repeated once again to completely remove the CdS core. The final Au tubes were obtained after centrifugation and thorough washing.

Scanning electron microscopy (SEM) measurement was carried out on a field-emission environmental scanning electron microscope operated at 15 kV (FEI, Quanta 200). Transmission electron microscopy (TEM) images were taken on a JEM-200 CX transmission electron microscope. Energy-dispersive X-ray (EDX) analysis was obtained on an EDAX incorporated in a H9000 high resolution transmission electron microscope (HRTEM). UV-Vis spectra were recorded on a Varian-cary1E UV-Vis spectrophotometer and FL spectra were recorded on an F-4500 fluorescence spectrophotometer (Hitachi). X-ray photoelectron spectrum (XPS) was obtained on an Axis Ultra equipment (Al Kα source, Kratos, England).

## 2 Results and discussion

Mercapto reagents have strong affinity with CdX (X=S, Se, Te) [27]. Therefore, we chose MEA to introduce positive charges to the surfaces of CdS nanorods. Figure 1(a) shows the TEM image of MEA capped CdS nanorods. The introduction of the amino groups and the alkyl groups were identified by FT-IR spectra as shown in Figure 1(b). If the CdS nanorods were not modified by MEA, there were very few Au-nanoparticles found on the surfaces of CdS nanorods after Au deposition as shown in Figure 1(c). Figure 1(d) shows the as-prepared CdS-Au composite nanorods by chemical reduction using MEA modified CdS nanorods. The surface of CdS nanorods was found to have a homogeneous layer of Au nanoparticles. From the enlarged dark field image in Figure 1(e), the diameter of Au nanoparticles was measured to be 3–4 nm. As all samples were washed with water thoroughly before reduction, all the Au nanoparticles should come from $AuCl_4^-$ ions that previously absorbed on CdS nanorods. Thus the size and quantity of Au nanoparticles were determined by the amount of pre-adsorbed $AuCl_4^-$ ions. A MEA-CdS surface with many positive charges would adsorb more negatively charged $AuCl_4^-$ ions by strong electrostatic interaction, whereas un-modified CdS nanorods only adsorbed $AuCl_4^-$ ions by weak van der Waals interaction. The less absorption of $AuCl_4^-$ ions resulted in less Au nanoparticles deposited on un-modified CdS nanorods. Therefore, the composition and

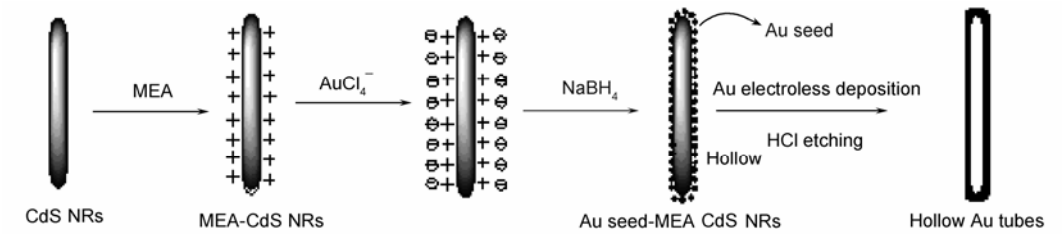


**Scheme 1** Schematic representation of the formation of CdS-nanorod/Au-nanoparticle composite and Au hollow tubes.

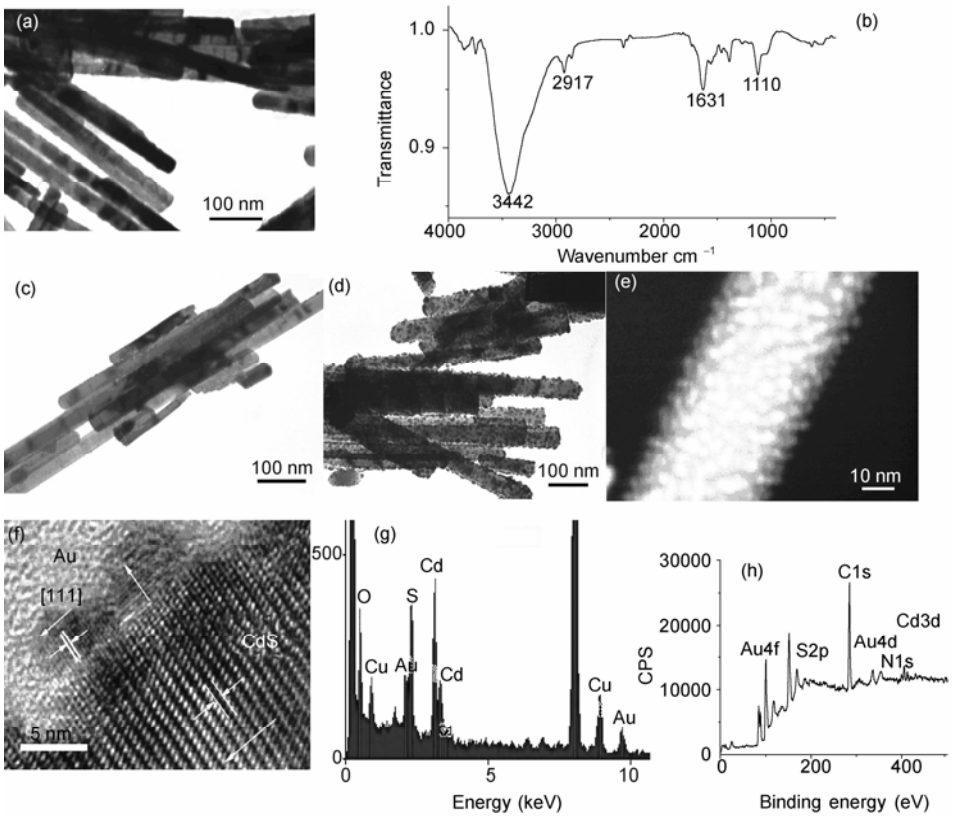


**Figure 1** (a) TEM image of MEA modified CdS nanorods; (b) IR spectrum of MEA modified CdS nanorods; (c) TEM image of unmodified CdS nanorods after Au deposition; (d) TEM image of MEA modified CdS nanorods after Au deposition; (e) an enlarged dark field image of CdS-MEA nanorods/Au-nanoparticles; (f) the corresponding HRTEM image of (e); (g) the corresponding EDS of (e); and (h) XPS spectrum for CdS-MEA nanorods/Au-nanoparticles.

morphology of the produced composites can be controlled by alternating the surface property of CdS nanorods.

From the HRTEM image of CdS-MEA/Au composite nanorods shown in Figure 1(f), the uniform and well-resolved lattice fringes were observed, indicating the crystalline structure for both CdS and Au. The distances of the lattice space of the CdS and Au were measured to be 0.67 nm and 0.24 nm, which were corresponding to the {001} crystal planes of hexagonal CdS and the {111} crystal planes of cubic Au crystal, respectively. From the EDX analysis of CdS-MEA/Au nanorods shown in Figure 1(g), the characteristic peaks of Au, Cd and S can be easily found (Cu signal comes from the copper grid). Figure 1(h) shows the XPS result of CdS-MEA/Au nanorods. The signals from Cd3d (405.8 eV), S2p (162.5 eV) and Au4f (84.8 eV) appeared. The characteristic peak of N1s (400.1 eV) that came from the amino groups of MEA was also found.

The Au nanoparticles on the surfaces of CdS nanorods were found to be able to act as the nucleation seeds to form thicker and continuous Au layer by further electroless deposition [28]. Figure 2(a) and (b) shows the TEM and SEM images of CdS/Au nanorods after Au electroless deposition. The diameter of Au nanoparticles increased to 6–7 nm. By contrast, those unmodified CdS samples only obtained a random Au deposition after the same reaction as shown in Figure 2(e), indicating that the pre-coated Au nanoparticles played key roles in forming continuous and homogeneous Au layers around the nanorods.

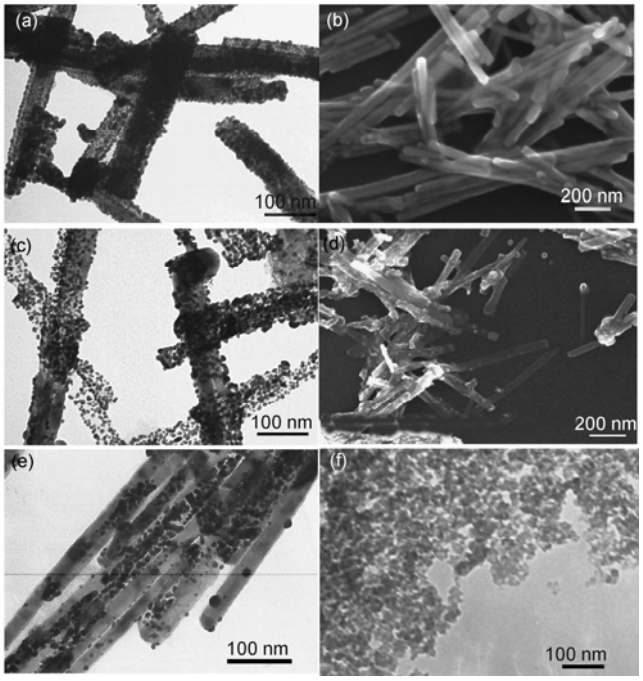


**Figure 2** TEM and SEM images of CdS-MEA/Au nanorods after Au electroless deposition ((a), (b)) and Au hollow tubes produced by HCl treatment ((c), (d)). (e) is the TEM image of unmodified CdS nanorods with Au nanoparticles after electroless deposition and (f) is the TEM image of the random Au nanoparticles produced by HCl treatment of CdS-MEA/Au nanorods without Au electroless deposition.

To testify the stability of the Au layer, we used 4.8 mol/L HCl solution to remove the inner CdS core. CdS can be dissolved by HCl with a concentration higher than 4 mol/L. Figure 2(c) shows the TEM image of the obtained tube-like Au hollow structures after HCl etching. Compared with the composite CdS/Au nanorods (Figure 2(a)), those Au tubes had much lower contrast in the center, indicating the absence of the solid CdS core. From the SEM image shown in Figure 2(d), we also found those Au hollow tubes had much lower contrast compared with the solid CdS/Au nanorods (Figure 2(b)). Some holes found at the open end of the tube further identified their hollow structure. Another fact should be pointed out that both the CdS/Au nanorods and the hollow Au tubes were very stable. They could retain their 1D structure even after a longtime ultra-sonication treatment. However, those CdS-MEA/Au-nanoparticle samples (without Au electroless deposition) collapsed to random Au nanoparticles during the same etching process (Figure 2(f)). This result verified the formation of stable and continuous Au shells on the external surfaces of CdS nanorods after Au electroless deposition.

Some reports have revealed that there are energy transfer between Au and CdS nano components [29]. In order to investigate the interaction between Au and CdS, we examined the luminescent properties of CdS-MEA/Au-nanoparticles. Figure 3 shows the fluorescence spectra of aqueous dispersion (1 mg/mL) of initial CdS nanorods, MEA modified CdS nanorods and CdS-MEA/Au nanorods, respectively (excitation at 360 nm). For initial CdS nanorods, there was an emission peak at 530 nm, which denoted the surface defect emission of CdS. After the surface modification, the intensity of this emission peak increased dramatically. This may be explained by the increase of the surface states by chemical modification. However, after the Au deposition, this emission peak decreased extremely. This emission quenching can be ascribed to the nonradiative pathway created by Au SPR (surface plasma resonance). The energy level of Au SPR is lower than the surface defect emission gap of CdS-MEA nanorods. Under the irradiation, the energy of excitons of CdS nanorods will transfer to Au SPR. This plasmon-exciton interaction that leads to the emission quenching of the CdS nanorods is quite similar to what Mokari reported [24]. However, our case is very different from Kotov's Au-CdTe samples, which exhibited an enhancement of luminescence intensity. The main reason is probably the difference in band gap between CdS and CdTe. The emission gap of CdS is higher than Au SPR, and energy will transfer from the exciton of CdS to Au. But the emission gap of CdTe is lower than Au SPR, energy tends to transfer reversely, which leads to the increase of the luminescence. We also noticed another report by Lin et al. [29]. They found that in Au(core)/CdS(shell) nanostructures, the emission intensity was also enhanced. They assumed that the excited electrons on Au surface by surface plasma wave transferred to the conduction band of the CdS shell and recombined with holes in the valence band. In their case, the internal Au core is the key factor of the energy transfer. However, in our case, Au nanoparticles exist on the surface of CdS, which leads to the energy transferring from CdS excitons to Au SPR, indicating that the plasmon-exciton interaction will be greatly influenced by the superstructure of the material. This characteristic should be helpful for tuning the band gap of metal-semiconductor composites and controlling their optical property.

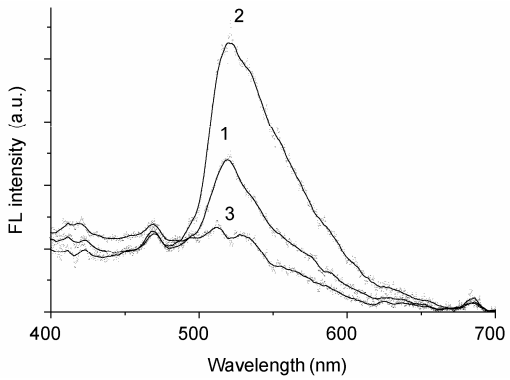


**Figure 3** FL spectra of aqueous dispersion of pure CdS nanorods (line 1), MEA modified CdS nanorods (line 2), and CdS-MEA/Au nanorods (line 3) (excitation at 360 nm).

It is known that the SPR band of spherical metal particles also greatly depends on their structure (solid or hollow) and the dielectric constant of the environment [30–32]. This factor can be used to tune the SPR band and design new types of electronic devices. Figure 4 shows the UV-Vis spectra of MEA-CdS nanorods, CdS-MEA/Au nanorods and Au tubes. The peak at 480 nm corresponded to the characteristic absorption of CdS nanorods. After Au nanoparticles' deposition, the peak had an obvious red-shift of 15–20 nm to 500 nm and was broadened, which can be explained by the interaction between the SPR of Au nanoparticles and CdS nanorods. After the removal of CdS core, the peak around 500 nm disappeared completely, indicating decomposition of the CdS component. Instead, a new broad band around 590 nm corresponded to the SPR of Au hollow tubes can be observed clearly. It was reported [30] that the SPR band of isolated Au nanoparticles with diameter of 50 nm appeared at around 530 nm with a sharp peak. However, our hollow Au tubes had a red-shift and an obvious broadened SPR peak. The Au nano-shells have been proved to be more sensitive to the environmental change compared with the isolated Au nanoparticles with a similar diameter [30]. Because the SPR intensity decays exponentially over a length scale of about 50 nm, the SPR for Au shell is determined by the dielectric constant of the adsorbing layer. Therefore, the high sensitivity of Au nano-shells to the environment and the high extinction coefficient in the red regime result in the red-shift and broadening of the SPR band compared with isolated Au nanoparticles [30–32].

## 3 Conclusions

In conclusion, a novel metal-semiconductor composite structure based on Au nanoparticles and CdS nanorods was successfully prepared by pre-modifying the nanorod surfaces with mercapto-ethylamine. The positive-charged surface of CdS nanorods acquired a uniform and dense coating of Au nanoparticles. Those Au nanoparticles on CdS nanorods could induce further electroless deposition to form a thicker Au layer. After dissolving the CdS core with HCl, stable hollow Au tubes were achieved. The energy transfer from the excitons of CdS to Au SPR was detected, which led to the quenching of the defect emission of CdS. Besides, the Au SPR band was dependent on the morphology of Au. This kind of novel 1D CdS/Au nanostructure and hollow Au tubes may have potential applications in catalysis, electronics and photo-electronics.

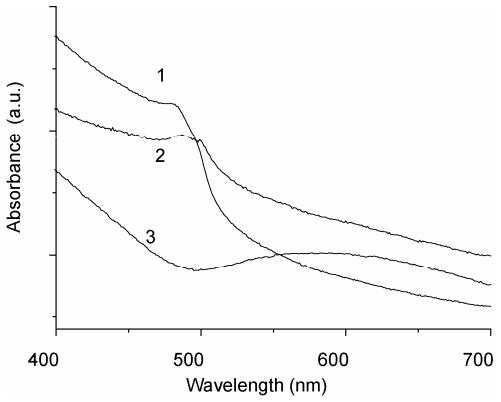


**Figure 4** UV-Vis spectra of the aqueous dispersion of pure CdS nanorods (line 1), CdS-MEA/Au nanorods (line 2) and hollow Au tubes after dissolving the inner CdS core by HCl (line 3).

*This work was supported by the National Natural Science Foundation of China* (*Grant No. 90406018*) *and Ministry of Science and Technology of China* (*Grant Nos. 2006CB0N0403 and 2007CB936202*).

1 Redl F X, Cho K S, Murray C B, et al. Three-dimensional binary superlattices of magnetic nanocrystals and semiconductor quantum dots. Nature, 2003, 423: 968–971
2 Burda C, Chen X, Narayanan R, et al. Chemistry and properties of nanocrystals of different shapes. Chem Rev, 2005, 105: 1025–1102
3 Xia Y N, Yang P D, Sun Y G, et al. One-dimensional nanostructures: Synthesis, characterization, and applications. Adv Mater, 2003, 15: 353–385
4 Duan X F, Huang Y, Agarwal R, et al. Single-nanowire electrically driven lasers. Nature, 2003, 421: 241–245
5 Carrillo A, Swartz J A, Gamba J M, et al. Noncovalent functionalization of graphite and carbon nanotubes with polymer multilayers and gold nanoparticles. Nano Lett, 2003, 3: 1437–1440
6 Ravindran S, Bozhilov K N, Ozkan C S. Self assembly of ordered artificial solids of semiconducting ZnS capped CdSe nanoparticles at carbon nanotube ends. Carbon, 2004, 42: 1537–1542
7 Liu L, Wang T, Li J, et al. Self-assembly of gold nanoparticles to carbon nanotubes using a thiol-terminated pyrene as interlinker. Chem Phys Lett, 2002, 367: 747–752
8 Osterloh F E, Martino J S, Hiramatsu H, et al. Stringing up the pearls: Self-assembly, optical and electronic properties of CdSe- and Au-LiMo3Se3 nanoparticle-nanowire composites. Nano Lett, 2003, 3: 125–129
9 Penner R M. Mesoscopic metal particles and wires by electrodeposition. J Phys Chem B, 2002, 106: 3339–3353
10 Wang S, Mamedova N, Kotov N A, et al. Antigen/antibody immunocomplex from CdTe nanoparticle bioconjugates. Nano Lett, 2002, 2: 817–822
11 Zanchet D, Micheel C M, Parak W J, et al. Electrophoretic and structural studies of DNA-directed Au nanoparticle groupings. J Phys Chem B, 2002, 106: 11758–11763
12 Maxwell D J, Taylor J R, Nie S. Self-assembled nanoparticle probes for recognition and detection of biomolecules. J Am Chem Soc, 2002, 124: 9606–9612
13 Colvin V L, Schlamp M C, Alivisatos A P. Light-emmiting-diodes made from cadmium selenide nanocrystals and a semiconducting polymer. Nature, 1994, 370: 354–357
14 Beecroft L L, Ober C K. Nanocomposite materials for optical applications. Chem Mater, 1997, 9: 1302–1317
15 Derfus A M, Chan W C W, Bhatia S N. Intracellular delivery of quantum dots for live cell labeling and organelle tracking. Adv Mater, 2004, 16: 961–966
16 Cao Y C, Jin R, Mirkin C A. Nanoparticles with Raman spectroscopic fingerprints for DNA and RNA detection. Science, 2002, 297: 1536–1540
17 Thomas K G, Kamat P V. Chromophore-functionalized gold nanoparticles. Acc Chem Res, 2003, 36: 888–898
18 Link S, El Sayed M A. Optical properties and ultrafast dynamics of

metallic nanocrystals. Ann Rev Phys Chem, 2003, 54: 331–366
19 Shipway A N, Katz E, Willner I. Nanoparticle arrays on surfaces for electronic, optical, and sensor applications. ChemPhysChem, 2000, 1: 18–52
20 Ma G H, He J, Rajiv K, et al. Observation of resonant energy transfer in Au : CdS nanocomposite. Appl Phys Lett, 2004, 84: 4684–4686
21 Yang Y, Nogami M, Shi J L, et al. Enhancement of third-order optical nonlinearities in 3-dimensional films of dielectric shell capped an composite nanoparticles. J Phys Chem B, 2005, 109: 4865–4871
22 Tang J, Birkedal H, McFarland E W, et al. Self-assembly of CdSe/CdS quantum dots by hydrogen bonding on Au surfaces for photoreception. Chem Commun, 2003, 18: 2278–2279
23 Granot E, Patolsky F, Willner I. Electrochemical assembly of a CdS semiconductor nanoparticle monolayer on surfaces: Structural properties and photoelectrochemical applications. J Phys Chem B, 2004, 108: 5875–5881
24 Mokari T, Rothenberg E, Popov I, et al. Selective growth of metal tips onto semiconductor quantum rods and tetrapods. Science, 2004, 304: 1787–1790
25 Lee J, Govorov A O, Dulka J, et al. Bioconjugates of CdTe nanowires and Au nanoparticles: Plasmon-exciton interactions, luminescence enhancement, and collective effects. Nano Lett, 2004, 4:2323–2330
26 Chu H B, Li X M, Chen G D, et al. Shape-controlled synthesis of CdS nanocrystals in mixed solvents. Cryst Growth Des, 2005, 5: 1801–1806
27 Ravindran S, Chaudhary S, Colburn B, et al. Covalent coupling of quantum dots to multiwalled carbon nanotubes for electronic device applications. Nano Lett, 2003, 3: 447–453
28 Jana N R, Gearheart L, Murphy C J. Evidence for seed-mediated nucleation in the chemical reduction of gold salts to gold nanoparticles. Chem Mater, 2001, 13: 2313–2322
29 Lin H Y, Chen Y F, Wu J G, et al. Carrier transfer induced photoluminescence change in metal-semiconductor core-shell nanostructures. Appl Phys Lett, 2006, 88: 161911
30 Sun Y G, Mayers B, Xia Y N. Metal nanostructures with hollow interiors. Adv Mater, 2003, 15: 641–646
31 Sun Y, Xia Y N. Increased sensitivity of surface plasmon resonance of gold nanoshells compared to that of gold solid colloids in response to environmental changes. Anal Chem, 2002, 74: 5297–5305
32 Jackson J B, Halas N J. Silver nanoshells: Variations in morphologies and optical properties. J Phys Chem B, 2001, 105: 2743–2746